Design and Development of Alkali Earth Metal-Based Nanoscale Material and their Potential Application in the Biomedical Field

Thesis submitted in partial fulfillment

For the Award of Degree

Doctor of Philosophy

BY

PRACHI SRIVASTAVA

SCHOOL OF BIOMEDICAL ENGINEERING

INDIAN INSTITUTE OF TECHNOLOGY BHU, VARANASI, 221005, U.P., INDIA

Roll No. 18021007

2023

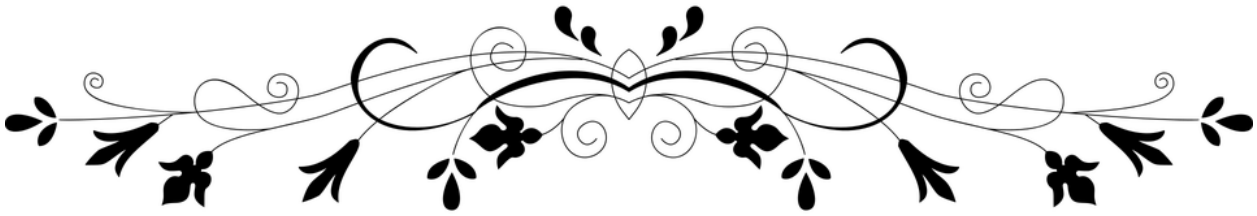

This Thesis work is dedicated to My Grandfather, Mr. Gyanendra Nath Verma & My Parents, Mr. Rajesh Kumar and Mrs. Savita Srivastava

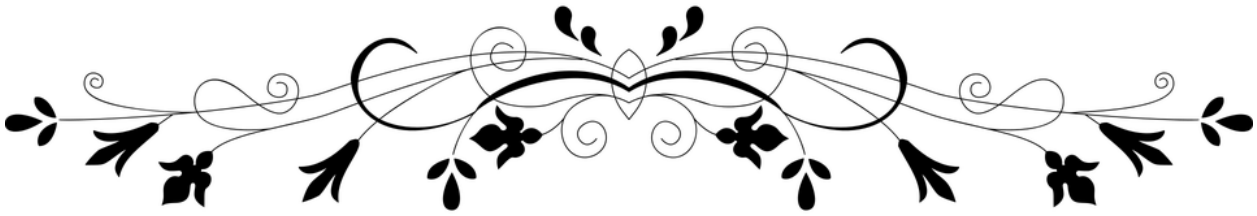

भारतीय प्रौद्योगिकी संस्थान
काशी हिन्दू विश्वविद्यालय

IIT INDIAN INSTITUTE OF TECHNOLOGY
BANARAS HINDU UNIVERSITY

CERTIFICATE

It is certified that the work contained in the thesis titled "**Design and Development of Alkali Earth Metal-Based Nanoscale Materials and their Potential Application in the Biomedical Field**" by **Prachi Srivastava** has been carried out under my supervision and that this work has not been submitted elsewhere for a degree.

It is further certified that the student has fulfilled all the requirements of Comprehensive Examination, Candidacy, and SOTA for the award of Ph.D. Degree.

Dr. Manoj Kumar
(Supervisor)
Department of Chemical Engineering & Technology,
Indian Institute of Technology,
(Banaras Hindu University),
Varanasi–221005, India

Dr. MANOJ KUMAR
Associate Professor
Department of Chemical Engg. & Techn.
IIT (BHU), Varanasi-221005

भारतीय प्रौद्योगिकी संस्थान
काशी हिन्दू विश्वविद्यालय
INDIAN INSTITUTE OF TECHNOLOGY
BANARAS HINDU UNIVERSITY

DECLARATION BY THE CANDIDATE

I, **Prachi Srivastava**, certify that the work embodied in this Ph.D. thesis is my own bonafide work and was carried out by me under the supervision of **Dr. Manoj Kumar** for a period from **July 2018 to August 2023** at the School of Biomedical Engineering, Indian Institute of Technology (Banaras Hindu University), Varanasi. The matter embodied in this thesis has not been submitted for any other degree/diploma award. I declare that I have faithfully acknowledged and given credit to the research workers wherever their works have been cited in my work in this thesis. I further declare that I have not wilfully copied any other's work, paragraph, text, data, results, etc. reported in the journals, books, magazines, reports, dissertations, thesis, etc., or available on websites and have not included in this thesis and have not cited as my own work.

Date: 29/08/2023

Place: IIT (BHU), Varanasi

Prachi
Prachi Srivastava

CERTIFICATE FROM THE SUPERVISOR

It is certified that the above statement made by the student is correct to the best of my knowledge.

Dr. Manoj Kumar

(Supervisor)

Department of Chemical Engineering & Technology,
Indian Institute of Technology
(Banaras Hindu University),
Varanasi–221005, India

Dr. MANOJ KUMAR
Associate Professor
Department of Chemical Engg. & Technology
IIT (BHU), Varanasi-221005

Coordinator of the School 28.08.23
समन्वयक/CO-ORDINATOR
जैव चिकित्सा अभियांत्रिकी स्कूल
SCHOOL OF BIOMEDICAL ENGG.
भारतीय प्रौद्योगिकी संस्थान (का.हि.वि.)
INDIAN INSTITUTE OF TECHNOLOGY (B.H.U.)
वाराणसी 221005/VARANASI-221005

भारतीय प्रौद्योगिकी संस्थान
काशी हिन्दू विश्वविद्यालय

IIT INDIAN INSTITUTE OF TECHNOLOGY
BANARAS HINDU UNIVERSITY

COPYRIGHT TRANSFER CERTIFICATE

Title of Thesis: "**Design and Development of Alkali Earth Metal-Based Nanoscale Materials and their Potential Application in the Biomedical Field**"

Candidate's Name: **Prachi Srivastava**

Copyright Transfer

The undersigned hereby assigns to the Indian Institute of Technology (Banaras Hindu University) Varanasi all rights under copyright that may exist in and for the above thesis submitted for the award of the Doctor of Philosophy degree.

Date: 29/08/2023

Place: IIT (BHU), Varanasi

Prachi

(Prachi Srivastava)

Note: However, the author may reproduce or authorize others to reproduce material extracted verbatim from the thesis or derivative of the thesis for the author's personal use, provided that the source and the Institute's copyright notice are indicated.

ACKNOWLEDGEMENT

Here I am, facing the end of a journey, and what a journey it has been. This is the time for farewells and words of gratitude, of thankfulness, and acknowledgment. I am deeply grateful to all the individuals and institutions whose support, guidance, and encouragement made the completion of this thesis possible.

First and foremost, with immense pleasure and gratitude, I would like to express my sincere appreciation toward my esteemed supervisor **Dr. Manoj Kumar**, Associate Professor, Department of Chemical Engineering and Technology, IIT(BHU), Varanasi, for his remarkable guidance, insightful feedback and unwavering support throughout my research journey. His expertise and dedication to work were instrumental in shaping this thesis work and guiding it toward new avenues.

Words cannot express my gratitude to **Dr. Sanjeev Kumar Mahto** (Associate Prof. School of Biomedical Engineering, IIT(BHU), Varanasi) and **Dr. Ashutosh Kumar Dubey** (Associate Prof, Department of Ceramic Engineering, IIT(BHU), Varanasi) as a part of my research progress evaluation committee. I could not have achieved my thesis goals without their insightful comments and suggestions. Their supreme knowledge and expertise supported me throughout achieving my thesis objective.

I would like to offer my special thanks to **Dr. Avanish Singh Parmar** (Associate Professor, Department of Physics, IIT(BHU), Varanasi), **Dr. Biplob Koch** (Associate Prof. of the Department of Zoology, Banaras Hindu University). **Dr. Sudip Mukherjee** (Assistant professor, School of Biomedical Engineering, IIT(BHU), Varanasi), **Dr. M.S. Muthu** (Associate professor, Department of Pharmaceutics Engineering and Technology, IIT(BHU), Varanasi) and **Prof. Ashok M. Raichur** (Professor, Department of Material

Engineering, IISC Bangalore). They always made time to listen to me and provided me with the facilities of his lab to carry out my research work.

I am also thankful to **Dr. Amaresh Kumar Sahoo** (Assistant Professor of the Department of Applied Science, IIIT-Allahabad) for his unparalleled supervision during my master's degree from IIIT-Allahabad. He always made time to listen and provide cautious advice and suggestions Whenever I needed it.

I owe my thanks to **Dr. Sanjeev Kumar Mahto** (coordinator), School of Biomedical Engineering, and **Prof. M.K Mondal** (Head), Department of Chemical Engineering & Technology, IIT (BHU) for encouraging and providing me with all the facilities to carry out my research work.

I am highly indebted to my Parents, **Mr. Rajesh Kumar** and **Mrs. Savita Srivastava**. I feel truly blessed and lucky to have parents like them. Everything that I achieved and wherever I am is only because of My parents, who sacrificed a ton and let go of their dreams so that I can achieve mine. No amount of words will be enough to tell how grateful I am to you. Thank you so much for your unconditional love and support.

I am deeply grateful and would like to convey my heartfelt gratitude to my friend **Vivek Kumar Verma**, my aunt **Mrs. Madhuri Srivastava**, and **my sisters**, **Ashwina Srivastava, Pallavi Srivastava, Preeti Srivastava**, and my whole family members, for being a constant source of encouragement and emotional support. They were there to listen and provide a helping hand whenever needed.

I am eternally grateful and most heartful thanks to my friend, **Dr Sumit Kumar**, for his useful advice and suggestions; I would like to express my deepest and heartfelt thanks to my senior, **Dr. Himanshu Kumar**, for his valuable support and guidance.

I would like to thank my seniors, **Shivesh Sabbarwal** and **Dr. Kedar Sahoo**, for their sincere guidance, cooperation, and motivation during the entire thesis work. I am also thankful to all my lab mates, **Mr. Vivek Kumar Verma**, **Mr. Anshuman Singh**, and **Ms. Rinki Verma**, for their valuable help and moral support throughout this journey.

I would like to thank my friends **Deepa Dehari, Abhishesh Kumar Mehta, Bindu Kumari, Mamta Singh**, and **Vivek Kumar Jaiswal**. They have always been a source of inspiration for me and have stood by my side at the most challenging times.

I would like to sincerely thank all DPGC members for their direct or indirect motivation and assistance from different corners during my research work at the institute. Also, I express my sincere thanks to all faculty members and non-teaching staff of the School of Biomedical Engineering, Indian Institute of Technology (BHU), for their continued help and cooperation in completing this dissertation work.

I am grateful to MHRD for providing financial support for my research. Their funding allowed me to carry out experiments and access critical research materials.

I cannot overstate the importance of the contributions made by the dedicated professionals who assisted me in this endeavor. I extend my thanks to CIF, IIT BHU, SATHI, BIONEST incubation center and for their technical assistance and guidance.

Lastly, I express my appreciation to all the participants who willingly took part in the studies conducted for this thesis. Without their cooperation, this research would not have been possible.

Date: 29/08/2023 (Prachi Srivastava)

Place: IIT (BHU), Varanasi

Table of Contents Page No.

Certificate……..iii
Declaration by the candidate and certificate by the supervisor…….iv
Copyright transfer certificate……...……..….v
Acknowledgment……vi-viii
Table of contents…….x-xv
List of figures…….xvi-xx
List of tables ……..….xxi
List of Abbreviations……..…….…….xxii-xiii
Preface …….…...xxiv-xxvi
Chapter 1…….....1-27
1.1 Introduction……..……1-2
1.2 Synthesis strategy of nanomaterials…….....2-4
1.3 Size control of nanomaterials……....4-5
1.4 Nucleation Mechanism and Involved Thermodynamics……..…….5-6
1.5 Concept of colloidal stability…….……...6-7
1.6 Size Restriction and Colloidal Stability (Kinetic and thermodynamic control) …….7
1.7 Application of nanomaterials in the biomedical field……...7-9
1.7.1 Drug Delivery……...…..…8
1.7.2 Imaging……...…..…..8
1.7.3 Biosensors and Diagnostics……..…….8
1.7.4 Theragnostic……...…….....9
1.7.5 Bioimaging and Photothermal Therapy……...……..9
1.7.6 Antimicrobial Applications…….....9
1.8 Common Bioimaging Techniques……...…..10-11
1.8.1 Bioluminescence imaging……..10
1.8.2 Fluorescence imaging…….....10-11
1.9 A brief overview of imaging agent /Fluorophore for optical imaging……..12-14
1.10 A brief overview of Conventional Bioimaging Agents and their disadvantages.13-15
1.10.1 Quantum dots……..…….13
1.10.2 Dye-doped silica nanoparticles…….…….…..14

1.10.3 Carbon nanomaterials…….…….....15
1.11 Fluorophore global market size……...…….17
1.12 Ideal bioimaging agent…….…….……...18
1.13 Mechanism of bacteria-killing……....18-19
1.14 Ideal antibacterial agent…….……..…....20
1.15 Alkali earth metal-based nanomaterial……...20-22
1.16 Magnesium-based nanomaterial in biomedical application ……...23-24
1.17 Magnesium-based nanomaterial as fluorophore…….….24-25
1.18 Problem statement defined……..26-27
Chapter 2 Literature review……...…….27-53
2.1 Mg Discovery and Its First Biomedical Application…….....31-32
2.2 Synthesis of magnesium-based nanomaterial……...….33-34
2.3 White light-emitting nanomaterial……...……..…35-37
2.4 Factor affecting properties and application of nanomaterial……...…….38-39
2.4.1 Morphology……..38
2.4.2 Particle size …… …….38
2.4.3 Surface area ……395
2.4.4 Stability…….39
2.5 Use of Model free methods for computation of activation energy……....40-41
2.6 Investigation of thermodynamic parameter……...….41
2.7 Computation of nucleation rate and interfacial energy of nanomaterial…….…..41-44
2.8 Biomedical Application……....…….45-50
2.8.1 Background……...……...45
2.8.2 Bioimaging and biosensing……..…46
2.8.3 Antibacterial agent……...…47
2.8.4 Drug delivery……...……..….48
2.8.5 Catalyst/Enzyme……...……..…....48-49
2.8.6 Wound Healing ……..…….49
2.8.7 Medical implant……..…….50
2.9 Problem statement…….…..…..50-53
2.10 Aim and Objective of the current work……..51-53

Chapter 3
Fluorescent Magnesium nanoclusters…….55-85
3.1 Introduction……...55-58
3.2 Experimental Section ……58-63
3.2.1 Material ……..…….58
3.2.2 Characterization…….…….59
3.2.3 Synthesis of FMNCs……..…….……..59-60
3.2.4 Optimization of FMNCs……60-61
3.2.5 Cell Culture and MTT Assay……...….61-62
3.2.6 Cell Imaging…….……..62
3.2.7 MALDI-TOF…….62-62
3.2.8 Fluorescence Lifetime…….…….…..63
3.2.9 Quantum Yield…….…….….63
3.3 Result and discussion ……...……64-84
3.3.1 Fluorescence spectroscopy and UV-Vis Spectroscopic characterization….64-68
3.3.2 Surface and Infrared Spectroscopy……...68-71
3.3.3 Size and Phase Analysis…….…..71-73
3.3.4 Lifetime Analysis…….74-78
3.3.5 Stability of FMNCs……..80-81
3.3.6 Application of FMNCs…….81-84
3.3.6.1 Cytocompability (MTT assay) and Bioimaging……...….82-83
3.3.6.2 Cell Imaging……...…83-84
3.4 Conclusion…….……85
Chapter 4
Nucleation Rate & Interfacial Energy for FMNCs ……...…….87-121
4.1 Introduction…….,…….87-90
4.2 Theoretical background for determination of kinetic parameters…… . 91-100
4.2.1 Thermogravimetric analysis…….……..91
4.2.2 Kinetic study…….91-97
4.2.3 Calculation of pre-exponential kinetic factor……...……97-98
4.2.4 Computation of Thermodynamic Barriers of MgNCs for Initiation of Random Nucleation……..….98-99

4.2.5 Computation of Nucleation Rate, Kinetic barrier, Thermodynamic barrier, and Interfacial energy……...……99

4.2.6 Computation of clusters atom present in one cluster by using TEM data……100

4.3 Experimental section ……..……..100-101

4.3.1 Chemical used……...100

4.3.2 Synthesis of MgNCs…….100

4.3.3 Characterization……....101

4.4 Results and discussion ……..…101-120

4.4.1 UV-Vis absorbance……..101-102

4.4.2 Size and phase analysis……102-103

4.4.3 Surface and infrared spectroscopy……...……..104-106

4.4.4 Prediction of reaction kinetics and corresponding pathways……...106-108

4.4.5 Calculation of Apparent Activation Energy concerning Reaction Conversion……..109-112

4.4.6 Prediction of pre-exponential kinetic factor as a function of conversions……...112

4.4.7 Calculation of thermodynamic parameter against the reaction progression..112-116

4.4.8 Dependency of nucleation rate in conversion and temperature……117-118

4.4.9 Variation of Interfacial energy with temperature and reaction progression ……118-120

4.5 Conclusion ……..……121

Chapter 5

Lysozyme Stabilized Mg Nanoclusters……...……..……..123-154

5.1 Introduction……...……123-125

5.2 Materials and Methods……..……125-130

5.2.1 Chemicals reagents…….……..125

5.2.2 Synthesis procedure……...125-126

5.2.3 Characterization…….……...126

5.2.4 Cell culture and incubation with Lyz-MgNCs for bioimaging application…..127

5.2.5 Cytotoxicity evaluation…….……127-128

5.2.6 Blood Compatibility Assay…….……..……128

5.2.7 Histopathology in rat……...….129

5.2.8 Clinical signs and body weight measurement …….…….…129-130

5.2.9 In vivo biodistribution of the Lyz-MgNCs in the healthy mice……...……130

5.2.10 Absolute Quantum Yield Measurement……...…..…130
5.3 Results and Discussion……..130-153
5.4 Stability of Lyz-MgNCs……....137-140
5.5 Application of Lyz-MgNCs……..….140-153
5.5.1 Cytocompatibility (MTT assay) and Bioimaging ……..140-141
5.5.2 Blood Compatibility assay……...……..……141
5.5.3 Histopathology Results……...……142-143
5.5.4 Clinical signs and body weight measurement ……...…….……143-144
5.5.5 Cell Imaging……...……....144
5.5.6 Confocal Z-stack analysis……...……...…145-150
5.5.7 In vivo biodistribution of the Lyz-MgNCs in the healthy mice……152-
5.6 Ethical Clearance ……..……...153
5.7 Conclusion ……..…...…..154
Chapter 6
Essential oil Mediated
Magnogel…….155-172
6.1 Introduction……155-156
6.2 Experimental section……..156-161
6.2.1 Material …….156
6.2.2 Synthesis of Magnogel……..157
6.2.3 Characterization…….157
6.2.4 Microbial culture……...158
6.2.5 Antimicrobial activity……158-159
6.2.6 Oxidative stress mesurment ……..159-160
6.2.7 Chorioallantois membrane (CAM) assay for angiogenic response ….……....160
6.2.8 CAM assay for antibacterial study ……...……..……..160-161
6.3 Physical Evaluation of the Magnogel……..…….……161
6.3.1 Organoleptic Properties……..……..……161
6.3.2 Spreadability test……..……161
6.3.3 pH Test……..……...161
6.4 Results and discussion ……...……...…161-170
6.4.1 CAM assay analysis…….…….166-167

6.4.2 Antimicrobial study analysis……...…..……..…..167-170
6.5 Conclusion ……..……172
Chapter 7
Conclusion and future work ……...……173-176
7.1 Conclusion…….173-175
7.2 Future work……...……176
References……177-216
APPENDIX……..217-236
Publications……..237-238
Permission from Central Ethical Committee……..……239
2

List of Figures

Figure no.	Figure caption	Page no.
Figure 1.1	Schematic representation of nanomaterial based on size, shapes, types, and surface modification	2
Figure 1.2	Schematic representation of top-down and bottom approach for the synthesis of nanomaterial	4
Figure 1.3	Flow diagram of different methods applied for the synthesis of nanomaterial.	4
Figure 1.4	Schematic illustration of the global fluorophore market	17
Figure 1.5	Possible pathways for bacteria cell Killing	19
Figure 1.6	Representation of work done in alkali metal	22
Figure 1.7	Inheritant properties of magnesium	24
Figure 1.8	Schematic representation of Mg properties as a fluorescent probe	25
Figure 2.1	Role of Magnesium Metal in the Biomedical Field	29
Figure 2.2	Characteristic features of Magnesium metal	33
Figure 2.3	Schematic Representation of Mg in Biomedical Application	45
Figure 3.1	The fluorescence emission spectra of FMNCs (30 mg/ml) and controls (Control 1: MgCl2 salt + BSA protein (31 mg/ml); Control 2: MgCl2 salt + ascorbic acid (8.37 mg/ml) at (a) The optimal excitation and emission spectra (λEx. 366 nm / λEm.450 nm) of FMNCs and control and its inset image shows aqueous FMNCs colloid under 366 nm excitation. (b) the excitation and emission spectra (λEx. 469 nm / λEx. 536 nm) of FMNCs and its control and its inset image shows aqueous FMNCs colloid under 469 nm excitation. (c) Excitation and emission spectra (λ Ex. 516 nm / λ Em. 565) FMNCs and its control (d) excitation and emission spectra of FMNCs and its control at λEx. 560 nm and λ Em620 and the inset image shows aqueous FMNCs colloid under 560 nm excitation.	65
Figure 3.2	(a) CIE chromaticity diagram of FMNCs shows the coordinate (0.30, 0.33) as the single emitter at 300 nm excitation. (b) The normalized photoluminescence intensity spectra of FMNCs at 300 nm excitation and the inset image shows lyophilized FMNCs powder with and without UV excitation (one-year-old) (c) Excitation wavelength-dependent broad emission spectra of	67

	FMNCs. (d) UV-Vis absorption spectra of native BSA and FMNCs	
Figure 3.3	a) FTIR spectra of FMNCs and BSA protein, (b) XPS Survey data, (c) Mg 2s, (d) S 2p	70
Figure 3.4	(a) HR-TEM image of the FMNCs at 20 nm scale bar (b) Particle size distribution curve, which was calculated using TEM image. (c) MALDI-TOF spectra of BSA (d) MALDI-TOF spectra of FMNCs	72
Figure 3.5	XRD spectra of BSA and FMNCs	73
Figure 3.6	(a) Fluorescence lifetime decay profile (λEx 496 nm/λ Em 564 nm) of FMNCs (b) Fluorescence lifetime decay profile (λEx 598 nm/λ Em 658 nm) of FMNCs (c) Fluorescence lifetime decay profile (λEx 496 nm/λ Em 564 nm) of Processed BSA (d) Fluorescence lifetime decay profile (λEx 598 nm/λ Em 658 nm) of Processed BSA	77
Figure 3.7	(a) Fluorescence spectra of FMNCs and Quinine sulfate as reference at 366 nm excitation value, under the same absorbance value (<0.5). (b) Fluorescence spectra of FMNCs against rhodamine 6G at 469 nm emission. (c) Indirect optical band gap energy of FMNCs. (d) Direct optical band gap energy of FMNCs.	79
Figure 3.8	(a) Photostability of FMNCs at different excitations (366, 469, 516 and 560) (b) ph. Dependent Fluorescence emission spectra at different pH. (6,8,10 and 12) Values, The pH. of the parent medium was 4.0	81
Figure 3.9	(a) Cell viability measurement, followed using MTT assay of HEK-293 cells treated with different concentrations of FMNCs (stock concentration 30 mg/ml). (b) Cell viability assay of FMNCs and control medium on MDA-MB-231 cells by MTT assay after incubation with different concentrations of stock solution for 24 hrs. These experiments are performed in triplicate and represented as the mean±SD	83
Figure 3.10	Multi fluorescent image of HaCaT cells incubated with FMNCs (1/10th of stock solution) (A) Ex. 472 nm / Em. Green (B) Ex. 472 nm / Em. Red (C) merged image (D) Bright-field image.	84
Figure 4.1	(a) UV-Vis absorption spectra of BSA and MgNCs, (b) HR-TEM image of the MgNCs at 50 nm scale bar inset Histogram with the distribution of MgNCs, (c) XRD of BSA and BSA capped MgNCs, (d) FTIR spectra of BSA and MgNCs.	103
Figure 4.2	XPS spectra of MgNCs (a) Mg 1s (b) Mg 2s (c) C1s (d) CD spectra of BSA and MgNCs	106

Figure 4.3	a) $z(\alpha)$ master plot for estimation of thermal decomposition reaction mechanism of MgNCs at 10°C/min (b) $z(\alpha)$ master plot for estimation of the thermal decomposition reaction mechanism of MgNCs at 15°C/min (c) $z(\alpha)$ master plot for estimation of the thermal decomposition reaction mechanism of MgNCs at 20°C/min.	108
Figure 4.4	Iso conversional models for kinetic analysis of MgNCs (a) KAS (b) FWO (c) Starink (d) Tang	109
Figure 4.5	(a) Comparison of apparent activation energies at all the conversions obtained from iso conversional models (b) Pre-exponential factor of MgNCs against conversions at all the three heating rates	112
Figure 4.6	(a) Plot between ΔG against Conversion at all three heating rates, (b) Plot between ΔH against Conversion at all three heating rates, (c) Plot between ΔS against Conversio at all three heating rates.	113
Figure 4.7	a) TGA and DTG curve of MgNCs at 10 °C/min heating rate (b) TGA and DTG curve of MgNCs at 15 °C/min heating rate (c) TGA and DTG curve of MgNCs at 20 °C/min heating rate	115
Figure 4.8	(a) Plot between nucleation rate and conversion(α) (b) Plot between nucleation rate and Temperature(K) (c) Plot between interfacial energy and conversion(α) (d) Plot between interfacial energy and Temperature (K).	120
Figure 5.1	The fluorescence emission spectra of Lyz-MgNCs and its control (without salt) (a) The optimal excitation emission spectra of Lyz-MgNCs and control at Ex- 366 / Em- 450 (b) The optimal excitation-emission spectra of Lyz-MgNCs and control at Ex- 469 / Em- 545 (c) The optimal excitation-emission spectra of Lyz-MgNCs and control at Ex- 560 /Em-628(d) UV spectroscopy of Lyz-MgNCs and native Lysozyme	132
Figure 5.2	Figure. 5.2 (a) HR-TEM image of the Lyz-MgNCs at 20 nm scale bar (b) Particle size distribution curve, which was calculated using TEM image. (c) Observed diffraction pattern and d-spacing of Lyz-MgNCs (d) XRD spectra of Lyz-MgNCs and native lysozyme protein.	134
Figure 5.3	(a) FTIR spectra of Lyz-MgNCs and native lysozyme protein (b) CD spectra of Lyz-MgNCs and native lysozyme protein.	136

Figure 5.4	XPS spectra of Lyz-MgNCs (a) Mg 1s (b) survey spectra (c) C 1s (d) O 1s	137
Figure 5.5	(a) Normalized fluorescence emission spectra of Lyz-MgNCs after addition of various concentration of freshly prepared NaCl solution at λEx 469 (b) fluorescence emission spectra at 469 excitaion of freshly prepared Lyz-MgNCs and one year old Lyz-MgNCs.	138
Figure 5.6	(a) pH. Dependent Fluorescence emission spectra at different pH. (5.8-11) Values at λEx 469 nm, (b) Photostability of Lyz-MgNCs at different excitations (366,469 and 560).	140
Figure 5.7	(a) Normalized fluorescence intensity of Lyz-MgNCs with different solvents at λEx 469 nm (b) Cytotoxicity assessment in U-87 MG cells using MTT assay (c) Hemocomtability test of Lyz-MgNCs in rat blood.	142
Figure 5.8	Histopathological appearance in H & E-stained rat organ sections of all groups; (a) Normal tissue without injecting nanocluster (control group); (b) Tissue appearance (3 hrs) after injecting nanocluster through tail vein injection (c) Tissue appearance (7 days) after injecting nanocluster through tail vein injection, (d) Tissue appearance (28 days) after injecting nanocluster through tail vein injection. Bar: 10 μm	143
Figure 5.9	Multifluorescent confocal image of U 87-MG cells incubated with Lyz-MgNCs (1/10 th of 12.4 stock solution) (a) Ex.366 /Em. 460 (b) Ex.472 nm / Em. Green (c) Ex. 472 nm / Em. Red (d) merged image.Bar 77.3μm	145
Figure 5.10	Z stack confocal images of U-87 MG cell incubated with Lyz-MgNCs (Ex. 366 nm, Em. blue). (a) = 0 μm. (b) = 2 μm. (c) = 4 μm. (d) = 6 μm. (e) = 8 μm. (f) = 10 μm. (g) = 12 μm. (h) = 14 μm. (i) = 16 μm. (j) = 18 μm.	147
Figure 5.11	Z stack confocal images of U-87 MG cell incubated with Lyz-MgNCs (Ex. 460 nm, Em. green). (a) = 0 μm. (b) = 2 μm. (c) = 4 μm. (d) = 6 μm. (e) = 8 μm. (f) = 10 μm. (g) = 12 μm. (h) = 14 μm. (i) = 16 μm. (j) = 18 μm.	149
Figure 5.12	Z stack confocal images of U-87 MG cell incubated with Lyz-MgNCs (Ex. 560 nm, Em. red) (a) = 0 μm. (b) = 2 μm. (c) = 4 μm. (d) = 6 μm. (e) = 8 μm. (f) = 10 μm. (g) = 12 μm. (h) = 14 μm. (i) = 16 μm. (j) = 18 μm.	151
Figure 5.13	Live animal fluorescent image after 3 h administration of saline in control mice and Lyz-MgNCs treated mice	153

Figure 6.1	(a) UV-Vis spectra of Magnogel (b) FTIR spectra of Magnogel and Essential oil	163
Figure 6.2	(a), Particle size distribution curve, which was calculated using TEM image (b) HR-TEM image of the Magnogel at 1μm scale bar	164
Figure 6.3	a), XPS spectra of Mg 1s (b) XPS spectra of O 1s (c) Physical image of Magnogel as supernatant (d) Spreadability of Magnogel	165
Figure 6.4	.CAM assay: (a-f). Growth of blood vessels treated with Magnogel at 0.035 μg/μl at 0.017 μg/μl,and untreated at 0h and 6h (g-i) The images are quantified with respect to length, junction, and size using ImageJ and Angiotool software. The black arrows indicate the change in blood vessels of the treatment groups at 0 h and 6 h time points. These experiments are performed in triplicate and represented as the mean±SD. No significant differences from UT embryos are observed (*p>0.05).	166
Figure 6.5	E. coli infected fertilized control eggs and Magnogel-treated eggs.	167
Figure 6.6	Spreadability antibacterial test of Magnogel with E. coli and S. aureus	168
Figure 6.7	Zone of inhibition seen due to the antibacterial action of Magnogel in E. coli bacteria (b) Relative antibacterial action with respect to conventional drug and control seen in histogram plot (c) Zone of inhibition seen due to the antibacterial action of Magnogel in S.aureus bacteria (d) Relative antibacterial action with respect to conventional drug and control seen in histogram plot	169
Figure 6.8	Spreadability plate test of Magnogel against candida albicans fungus	169
Figure 6.9	Zone of inhibition seen due to the antibacterial action of Magnogel in Candida albicans fungus (D; drug , M; Magnogel ,E ; essential oil , B; bacterial cellulose) (b) Relative antibacterial action with respect to conventional drug and control seen in histogram plot	170
Figure 6.10	a) NBT assay for Magnogel after incubation for 1 hour with bacterial cells (b) Histogram plot depicting the amount of ROS produced during NBT assay at MIC concentration of E. coli and S. aureus	171

List of Tables

Table no.	Table caption	Page no.
Table 1.1	Drawbacks of conventional imaging agents	16
Table 2.1	List of metals used in biomedical application	30-31
Table 2.2	Synthesis method of metallic Magnesium nanoparticles via a different route	35
Table 2.3	Literature based on white light emission generation and its application	37
Table 3.1	Fluorescence life time of BSA and Processed BSA	75
Table 4.1	Calculated Activation energy using different models	110
Table 4.2	Calculated Thermodynamic parameters for different heating rates (10 ° C/min, 15 ° C/min, 20 ° C/min)	116

List of Abbreviations and Symbols

Abbreviation	Nomenclature
NPs	Nanoparticles
NCs	Nanoclusters
FMNCs	Fluorescent metallic nanoclusters
Lyz-MgNCs	Lysozyme-templated magnesium nanoclusters
NBT	Nitrotetrazolium blue
CAM	Chorioallantoic membrane
IVIS	In vivo imaging system
CT	Computed tomography
MRI	Magnetic resonance imaging
SPECT	Single-photon emission computed tomography
MALDI-TOF	Matrix-assisted laser desorption/ionization
CTCF	Corrected total cell fluorescence
GFP	Green fluorescent protein
QDs	Quantum dots
FRET	Förster resonance energy transfer
BSA	Bovine albumin serum
ROS	Reactive oxygen species
MIC	Minimum inhibitory concentration
MBC	Minimum bactericidal concentration
WLE	White light emission
CIE	Commission internationale de l'éclairage
KAS	Kissinger-Akahira-Sunose
FWO	Flynn-Wall-Ozawa
Vyazovkin AIC	Vyazovkin Advanced isoconversional
TGA	Thermogravimetric analysis
β	Heating rate
α	Conversion point
J0	Kinetic barrier of nucleation
J	Nucleation rate
T_P	Peak temperature
K_B	Boltzmann constant
$E\alpha$	Activation energy of nucleation
$A\alpha$	Pre-exponential kinetic factor
ΔH	Change in enthalpy
ΔG	Change in Gibbs free energy
ΔS	Change in entropy
$f(\alpha)$	Differential function
$g(\alpha)$	Integral function
Exp ($\Delta G/RT$)	Thermodynamic barrier
M0	Initial weight of MgNCs before TGA
Mf	Final weight of MgNCs after TGA
R	Universal gas constant
$Z(\alpha)$	Product of differential and integral function
h	Plank constant
FWHM	Full-width half maxima

XPS	X-ray photoelectron spectroscopy
XRD	X-ray diffraction
FTIR	Fourier-transform infrared spectroscopy
HRTEM	High-resolution transmission electron microscopy
CD	Circular dichroism

Preface and Thesis Organization

Recent advancements in nanoscience and nanotechnology have opened up new prospects for developing metallic nanomaterials, which are biocompatible with improved sensitivity and specificity for the healthcare system. Metallic nanoclusters have emerged as promising nanoscale materials with numerous applications, but due to the existence of long-term toxicity during in-vivo studies on noble metals, research in recent years has focused on developing more biocompatible materials. As a relatively safe material with a broad range of applications, magnesium emerges as a noble platform for fabricating some new class of therapeutic tools for potential applicability in bioimaging, eradication of multiple drug-resistant pathogens, development of wound caring material for accelerated healing, and artificial mimetic enzymes.

In this thesis, we discussed the simple, facile synthesis route and surface functionalization strategies that enable the precise control of the nanomaterial's size, morphology, and surface properties. In this regard, we exclusively synthesize ultrasmall magnesium nanoclusters and magnesium-based gel via a biogenic approach for bioimaging and antimicrobial application. These nanoscale materials are typically composed of magnesium and various surface coatings such as lysozyme, BSA, and essential oil, which makes them suitable for in vivo imaging applications and against microbial infection, minimizing adverse effects on living systems.

Furthermore, we performed extensive post-characterization studies such as confocal microscopy, in-vivo imaging system in rodents, in-vitro biocompatibility and hemocompatibility, in-vivo biocompatibility, broad range pH stability, ionic strength, quantum yield (relative and absolute), photostability and solvometric effect to affirm their candidature toward cell labeling and imaging purposes. while essential oil-derived

magnesium gels were used to investigate in-vitro and in-vivo antimicrobial responses in a broad range of bacterial and fungal cells, along with CAM assay in chicken eggs to interrogate its biocomtabilty and angiogenic response. In contrast, despite spanning several decades, plenty of research was focused on calculating the nucleation rate of ultra-small clusters in the low-temperature range (20°C to 100°C), but in the high-temperature range, there was no engineered technology to calculate the same mathematically. To address this issue, we employed thermogravimetric (TGA) analyses to calculate the nucleation rate of ultra-small clusters in the high-temperature range and the corresponding conversions. In addition, we address the challenges and future prospects of magnesium-based nanomaterials in the biomedical field, including targeting efficiency and long-term biodistribution. As research in this area continues to progress, it is expected that these challenges will be addressed, leading to the development of even more sophisticated magnesium-based nanomaterial with improved capabilities and therapeutic functionalities.

The current thesis work is divided into seven chapters.

Chapter 1 of the thesis covered a detailed description of nanoscience and nanotechnology, along with their design and development strategy. It also provides insight into their multidimensional applications in healthcare-related fields. This chapter provides the details of the global market involved in commercial dye and other nanosystems available for bioimaging. This chapter also provides a detailed discussion of mechanisms involved in antibacterial properties with the effect of thermodynamic parameters and kinetic parameters on size control and their colloidal stability.

Chapter 2 This chapter includes the role and advantage of magnesium-based nanomaterial over conventional metals, followed by the development strategy of metallic magnesium nanoclusters and their multimodal application in various fields. This chapter also gives

insight into the origin of white light emission and its prospective application. In contrast, this study also addresses the challenges associated with determining the nucleation rate and interfacial energy at elevated temperatures, as well as the corresponding conversions. The literature survey also addresses the antibacterial capabilities of the nanoparticles that were synthesized.

Chapter 3 Explains a facile one-pot novel technique to synthesize multifluorescent metallic magnesium nanoclusters by utilizing BSA protein and ascorbic acid as reducing and capping agents, respectively. The prepared clusters exhibited tunable fluorescence, high quantum yield, excellent photostability, wide-range pH, and ionic strength tolerability. These multifunctional properties of magnesium nanoclusters are availed in labeling HaCaT cell lines with negligible toxicity.

Chapter 4 of the thesis reports a novel strategy to estimate various parameters such as activation energy, nucleation rate, interfacial energy, and thermodynamic parameters of metallic magnesium nanoclusters using non-isoconversional thermogravimetric models at high temperatures. The Vyazovkin AIC method was utilized to estimate activation energy, which was found to be 159.56 kJ/mol. In this work, we proposed four different models for the computation of nucleation rate and interfacial energy.

Chapter 5 provides the one-pot facile synthesis of multifluorescent metallic magnesium nanoclusters using model protein lysozyme. The prepared clusters exhibit negligible cytotoxicity, excellent water dispersibility, eminent photostability, and high absolute quantum yield. Besides the in vitro study, this chapter includes in-vivo imaging, hemocompatibility assay, and in-vivo toxicological study.

Chapter 6 This chapter reported the biogenic approach to synthesizing magnesium gel using peppermint essential oil. This is the first kind of report on the generation of metallic

magnesium-based gel by simple one-pot technique. Prepared gel utilized to combat clinically relevant pathogens bacteria such as *E. coli*, *S. aureus*, and candida albicans (fungus). The biocompatibility and angiogenic response of the prepared gel were examined using CAM assay.

Chapter 7 of the thesis summarizes the whole study along with the future prospects of prepared nanoclusters in various fields. The composition reported in this study primarily focused on developing novel nanoplatforms for various applications by functionalizing them with different capping agents. The current work is envisioned to contribute significantly in the areas of science, engineering, and nanomedicine with targeted drug delivery.